Polynomial-based Inertia Ratio Controller Design for Vibration Suppression in Two-Mass System

Yue Qiao
Univ. of Michigan-Shanghai Jiao Tong Univ. Joint Institute,
Shanghai Jiao Tong University,
Shanghai, P. R. China
Email: qiaoyue.2000@163.com

Lin Zhou
Univ. of Michigan-Shanghai Jiao Tong Univ. Joint Institute,
Shanghai Jiao Tong University,
Shanghai, P. R. China
Email: automanzl@gmail.com

Chengbin Ma
Univ. of Michigan-Shanghai Jiao Tong Univ. Joint Institute,
Shanghai Jiao Tong University,
Shanghai, P. R. China
Email: chbma@sjtu.edu.cn

***Abstract*—In this paper, a polynomial-based design of inertia ratio controllers is discussed for the vibration suppression in two-mass system. A tradeoff relationship is shown to exist between damping and robustness performances in the control problem. A desirable inertia ratio of 5/16 is derived at which IP control provides a proper damping. Then two approaches for the control of equivalent inertia ratio are discussed without/with load velocity feedback. "Resonance ratio control" is capable of providing a sufficient damping for large inertia ratios by using only drive velocity feedback. However, a negative derivative gain is necessary, which leads to a poor robustness. By using both drive and load velocity feedback, the equivalent inertia ratio can be exactly specified as 5/16. The proposed "inertia ratio controller" design shows an obvious improvement in terms of both damping and robustness performances. All the experimental results validate the polynomial-based theoretical analysis and controller design. The demonstrated generality and the explicit expression of damping indicate the promising prospect of the polynomial-based controller design for solving more complicated control problems.**

I. Introduction

The fundamental trend of the electrification of drive systems is now expanding from industry to new areas such as alternative energy systems including electric vehicles and wind turbine generators [1][2]. The rapid and accurate response of electric motor greatly enhances drive system performance. However, the higher control bandwidth makes it easy to excite mechanical resonance. This vibration suppression control problem can be found in many electromechanical systems from traditional systems such as steel rolling mills and elevators to the above new applications. These electromechanical systems are usually modeled as multi-mass systems, while the control of two-mass systems can give a good starting point and general results for dealing with more complicated systems.

In the typical benchmark two-mass control problem, only the velocity of drive side is assumed measurable, whereas driving torque, load torque and the velocity of load side are not measurable [3][4]. The designed controller needs to control the velocity of the load side within well-suppressed vibrations by using only the velocity feedback of drive side. Various approaches have been proposed for the two-mass system control during the past decade such as the feedback of imperfect derivative of torsional torque estimated by a disturbance observer [3], a two-degree-of-freedom control structure using an observer-based state feedback compensator [5], μ-synthesis based on a descriptor form representation [6], a series anti-resonance finite-impulse response compensator [7], independent design of velocity control and vibration suppression control [8] and pole-placement-based PI/PID controller design [9]. A comparative study of different control structures for a two-mass electrical drive system is discussed in [10]. Intelligent control has also been applied in the two-mass control problem using fuzzy and neural network approaches [4][11]-[13].

It is well-known that low-order PID controllers and their modifications are predominant in electric drive industry. Continuous improvement on low-order controller design would significantly contribute to real engineering applications. Besides the well-established classical and modern control design, there exists an alternative approach called algebraic design using polynomial expressions, i.e., polynomial method. In the approach, because controller is designed based on the closed-loop characteristic polynomial, a general controller design and discussion are possible. In addition, the structure of controller is defined at the beginning. The controller parameters are then determined by specifying so-called characteristic ratios and generalized time constant. Therefore, the polynomial method is suitable for being used as a general approach to design low-order controllers.

More specifically, an essential issue for the controller design of two-mass system is to achieve a balanced tradeoff between damping and robustness performances, as explained in following sections. A controller design method that is capable of explicitly including the factor of damping would be highly desirable for vibration suppression purpose. It was reported that in polynomial method the assignment of characteristic ratios has a strong co-relationship with the damping of a closed-loop system. The transient response can also be addressed using characteristic ratios and generalized time constant [14][15]. Naslin empirically observed these relationships in 1960s [16]. Manabe proposed the Coefficient Diagram Method (CDM) based on Naslin's findings and the Lipatov-Sokolov stability criterion [17]. In CDM, the nominal assignment of characteristic ratios is proposed as $[2.5,\ 2,\ 2, \ldots]$ for smooth time responses.

This paper systematically applies the polynomial method in a challenging benchmark engineering problem, the vibration

978-1-4799-0224-8/13/$31.00

suppression in two-mass system. Using the frequency response of the normalized two-mass model, it is explained that the inertia ratio q directly relates to the difficulty of the controller design. A larger value of q corresponds to a stronger tendency of pole-zero cancellation. For the simple IP control, 5/16 is shown to be a desirable inertia ratio at which a balanced tradeoff between damping and robustness can be achieved. Consequently, for a system with a larger q, virtually reducing of q through a specific controller structure can be considered in order to avoid the pole-zero cancellation. Two approaches are then discussed for the control of the equivalent inertia ratio for the two-mass system without and with load velocity feedback, respectively.

II. Experimental Two-Mass System

The two-mass system can be emulated by using a laboratory torsion test bench. As shown in Fig. 1, the drive side and load side of the torsion system are connected with a torsional shaft. Drive torque is transmitted from drive servomotor to the shaft by gears with a gear ratio of 1:2. The torsion system can be modeled as a two-mass system, in which two masses are connected with a non-stiff coupling shaft [see Fig. 2]. The transfer function between driving torque T_m and angular velocity of drive side ω_m can be written as

$$P(s) = \frac{\Omega_m(s)}{T_m(s)} = \frac{s^2+\omega_a^2}{J_m s(s^2+\omega_r^2)}, \tag{1}$$

in which

$$\omega_r = \sqrt{K_s\left(\frac{1}{J_m}+\frac{1}{J_l}\right)} \text{ and } \omega_a = \sqrt{\frac{K_s}{J_l}}, \tag{2}$$

where K_s is the spring coefficient, while J_m and J_l are the inertias of the drive and load sides, ω_r and ω_a are the resonance frequency and anti-resonance frequency, respectively.

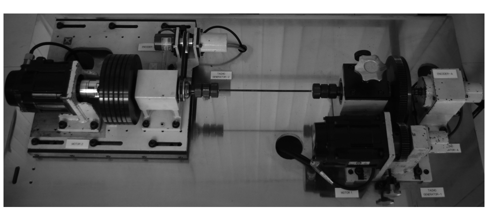

(a)

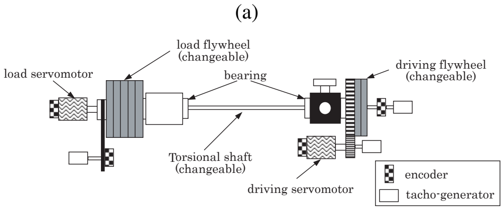

(b)

Fig. 1. Experimental setup of the torsion test bench.

For a generalized discussion, Eq. (1) can be normalized by replacing the Laplace operator s with s^*=s/ω_a, i.e.,

$$P(s^*) = \frac{q}{J_m}\frac{1}{\omega_a}\frac{s^{*2}+1}{qs^{*3}+s^*}, \tag{3}$$

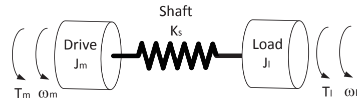

(a)

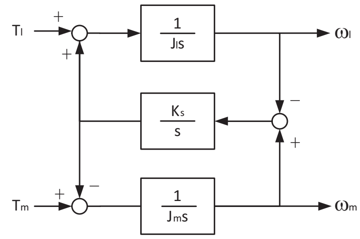

(b)

Fig. 2. The modeling of two-mass system. (a) Model. (b) Block diagram.

where q is the inertia ratio defined as the ratio of drive inertia to total inertia

$$q = \frac{J_m}{J_m+J_l}. \tag{4}$$

The normalized two-mass system model can be further simplified as

$$P_n(s^*) = \frac{\Omega_m(s^*)}{T_m(s^*)} = \frac{s^{*2}+1}{qs^{*3}+s^*}, \tag{5}$$

for which the normalized resonance frequency and anti-resonance frequency are

$$\omega_r^* = \frac{1}{\sqrt{q}},\ \omega_a^* = 1, \tag{6}$$

respectively. It is straightforward from the Laplace transform of time-scaled functions that the real response is sped up by a factor of ω_a. Based on Eq. (6), the two resonance frequencies, ω_r^* and ω_a^* become close when the inertia ratio q increases, i.e., the tendency of pole-zero cancellation. It is well-known that the pole-zero cancellation leads to poor robustness of a closed-loop control system [18].

On the other hand, with the placement of a load velocity sensor, the nonminimum-phase zeros in Eq. (5) can be eliminated. Because the normalized transfer function between load velocity ω_l and drive torque T_m is

$$\frac{\Omega_l(s^*)}{T_m(s^*)} = \frac{1}{qs^{*3}+s^*}, \tag{7}$$

in which the tendency of pole-zero cancellation is avoided.

III. Desirable Inertia Ratio

A desirable inertia ratio of the two-mass system for the polynomial-based controller design has been discussed [19]. Here, the desirable inertia ratio is re-examined and experimentally verified using a simple IP structure. As shown in Fig. 3, unlike the conventional PI controllers, a modified structure called setpoint-on-I-only structure is adopted to smooth the discontinuity of the reference command ω_r by the integral controller, which is widely used in servo drive industry [20]. The closed-loop transfer function for the IP control is

$$G_n(s^*) = \frac{K_i^*(s^{*2}+1)}{qs^{*4}+K_p^*s^{*3}+(1+K_i^*)s^{*2}+K_p^*s^*+K_i^*}. \tag{8}$$

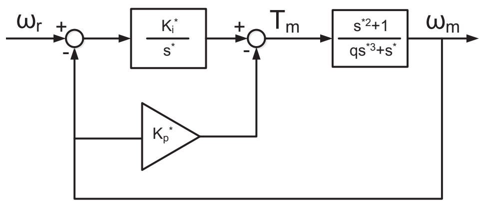

Fig. 3. Block diagram of IP velocity control of the normalized two-mass system.

Then, the control parameters are determined by applying the nominal characteristic ratio assignment [2.5, 2, 2, ...] in polynomial method. Based on Eq. (8), the characteristic ratios can be calculated as follow from the definition [14].

$$\gamma_1 = \frac{K_p^{*2}}{K_i^*(1+K_i^*)}\ \gamma_2 = \frac{(1+K_i^*)^2}{K_p^{*2}}\ \gamma_3 = \frac{K_p^{*2}}{q(1+K_i^*)}, \quad (9)$$

Unlike γ_1 and γ_2, γ_3 is also determined by the value of the inertia ratio q. Since the low-index characteristic ratios have a dominant influence, a straightforward strategy is to primarily guarantee γ_1 and γ_2. Let $\gamma_1 = 2.5$ and $\gamma_2 = 2$ in Eq. (9), K_p^* and K_i^* are determined as

$$K_p^* = \frac{5}{4\sqrt{2}}, \quad K_i^* = \frac{1}{4}, \quad (10)$$

and thus γ_3 is smaller than two when

$$q > \frac{5}{16} = 0.3125. \quad (11)$$

The real controller parameters K_p and K_i can be calculated as follows by comparing Eq. (5) with Eq. (3)

$$K_p = K_p^* \frac{J_m \omega_a}{q}, \quad K_i = K_i^* \frac{J_m \omega_a^2}{q}. \quad (12)$$

The experimental results of the IP control is shown in Fig. 4. Due to the existence of a 1:2 gear ratio between the drive and load sides, ω_l is half of ω_m. A step disturbance torque generated by the load servo motor is applied at 1 sec. It can be seen that a sufficient damping is provided when $q \le 5/16$ (see Fig. 4(a)(b)), while the step responses become oscillatory at larger q's (see Fig. 4(c)(d)). An inertia ratio q equals to 5/16 could be considered desirable at which γ_3 takes its nominal value, two. When q is smaller than 5/16, the system is overdamped (i.e., $\gamma_3 > 2$). Larger q's lead to insufficient damping (i.e., $\gamma_3 < 2$). For the cases with large q's, a control structure can be designed to virtually lower the real inertia ratio, as discussed in the following sections.

IV. Inertia Ratio Controller Design

A. *Without load velocity feedback*

The structure of so-called "resonance ratio control" in Fig. 5 can be used to control the equivalent inertia ratio of the two-mass system [8]. By using the polynomial method, its five controller parameters, K_p^*, K_i^*, K^*, K_d^* and T_d^* can be exactly determined. The low-pass filter $1/(T_d^* s^* + 1)$ is mainly introduced for the real implementation of the derivative term $K_d^* s^*$. By neglecting the low-pass filter, the transfer function between $T_m^{'}$ and ω_m can be written as

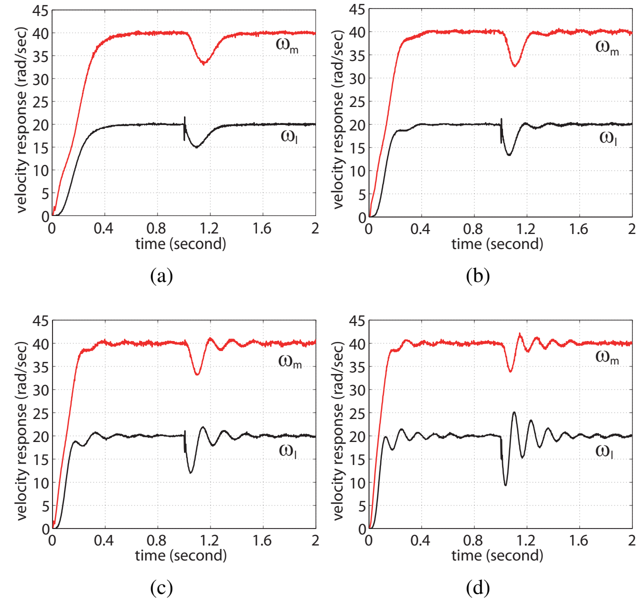

Fig. 4. IP control. (a) $q = 0.3612$. (b) $q = 0.5254$. (c) $q = 0.6752$. (d) $q = 0.7966$.

$$\frac{\Omega_m(s^*)}{T_m^{'}(s^*)} = \frac{1}{1-K^*+K_d^*} \frac{s^{*2}+1}{\left[\frac{(1-K^*)q+K_d^*}{1-K^*+K_d^*}\right] s^{*3} + s^*}, \quad (13)$$

where the equivalent inertia ratio $q^{'}$ is

$$q^{'} = \frac{(1-K^*)q + K_d^*}{1-K^*+K_d^*}. \quad (14)$$

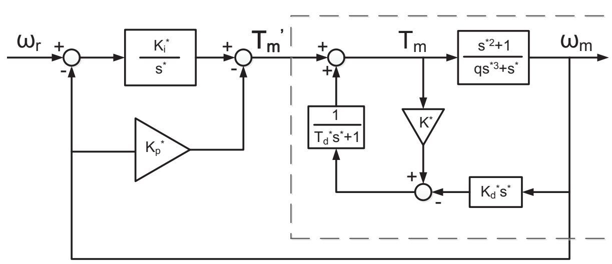

Fig. 5. Block diagram of "resonance ratio control".

The closed-loop transfer function in Fig. 5 is

$$G_n(s) = \frac{K_i^*(T_d^* s^* + 1)(s^{*2}+1)}{a_5 s^{*5} + a_4 s^{*4} + a_3 s^{*3} + a_2 s^{*2} + a_1 s^* + a_0}, \quad (15)$$

where

$$\begin{aligned} a_5 &= q T_d^*, \\ a_4 &= q + K_d^* - qK^* + K_p^* T_d^*, \\ a_3 &= T_d^* + K_p^* + K_i^* T_d^*, \\ a_2 &= 1 - K^* + K_d^* + K_i^* + K_p^* T_d^*, \\ a_1 &= K_p^* + K_i^* T_d^*, \\ a_0 &= K_i^*. \end{aligned} \quad (16)$$

Applying the nominal characteristic ratio assignment [2.5, 2, 2, 2], the coefficients in Eq. (16) can be solved using

$$a_n = \frac{\tau^n}{\gamma_{n-1}\gamma_{n-2}^2 \cdots \gamma_1^{n-1}} a_0. \tag{17}$$

In Eq. (16), because

$$\frac{a_5}{q} + a_1 = a_3, \tag{18}$$

then

$$\frac{\tau^5}{2^6 \cdot 2.5^4 \cdot q} K_i^* + \tau K_i^* = \frac{\tau^3}{2 \cdot 2.5^2} K_i^*. \tag{19}$$

Therefore, a positive τ is solely determined by q

$$\tau = 10\sqrt{q - \sqrt{q^2 - 0.25q}}. \tag{20}$$

Then all the other controller parameters can be simultaneously calculated as follows

$$\begin{aligned} K_i^* &= \frac{2500q}{\tau^5} T_d^*, \\ K_p^* &= (\tau - T_d^*) K_i^*, \\ K^* &= 1 + \frac{\tau^4 - 50\tau^2 + 125}{125(1-q)} K_i^*, \\ K_d^* &= \left(\frac{\tau^2}{2.5} - 1\right) K_i^* + K^* - K_p^* T_d^* - 1. \end{aligned} \tag{21}$$

For the fifth-order characteristic equation Eq. (16) under the nominal characteristic ratio assignment and with the determined τ in Eq. (20), its five poles are

$$\frac{-5.56 \pm 6.40i}{\tau}, \quad \frac{-3.02 \pm 1.76i}{\tau}, \quad \frac{-2.84}{\tau}, \tag{22}$$

respectively. In order to have a smooth transient response, the zero $z_1 (= -1/T_d^*)$ added by the low-pass filter $1/(T_d^* s + 1)$ needs to be properly located (see Eq. (15)). Suppose z_1 is α times of the real part of the leftmost roots $r_{1,2}$, i.e.,

$$T_d^* = \frac{\tau}{5.56\alpha}. \tag{23}$$

As shown in Fig. 6 at a large q(=0.75), the smooth step response at $\alpha = 5$ indicates an improved damping by the "resonance ratio control" (see Fig. 6(d)). Similarly, the real controller parameters can be calculated using Eqs. (12)(24).

$$K = K^*, \quad K_d = K_d^* \frac{J_m}{q}, \quad T_d = \frac{T_d^*}{\omega_a}. \tag{24}$$

Due to the existence of the first-order low-pass filter, there is no explicit representation of the equivalent inertia ratios for the "resonance ratio control". However, the quasi-equivalent inertia ratios calculated using Eq. (14) are still found to close to 5/16, as shown in Fig. 7(a). Meanwhile, the normalized derivative gain K_d^* is always negative for large q's, i.e., the positive feedback of the D control signal and thus a poor robustness (see Fig. 7(b)).

The experimental results are shown in Fig. 8. For the "resonance ratio control" structure, it is necessary to have a negative derivative gain (i.e., phase-lag) in order to provide a sufficient damping when q is large. However, the required robustness performance is largely ignored. In the benchmark two-mass control problem, it is assumed that only the velocity

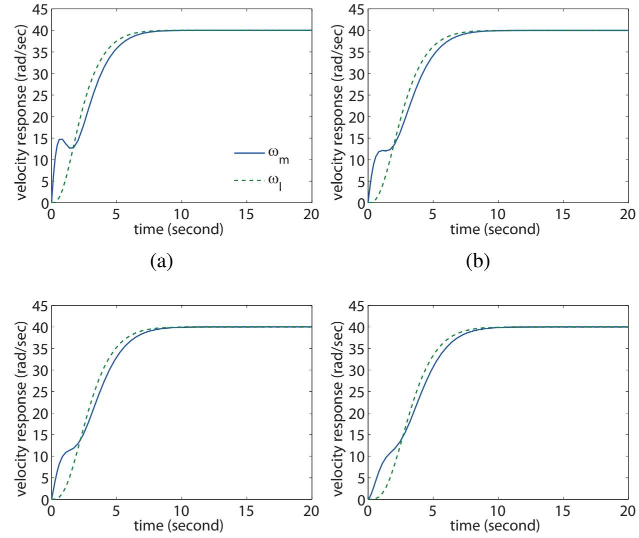

Fig. 6. Step responses of the "resonance ratio control" under various zero assignments (q=0.75). (a) $\alpha = 1.1$. (b) $\alpha = 1.5$. (c) $\alpha = 2.0$. (d) $\alpha = 5.0$.

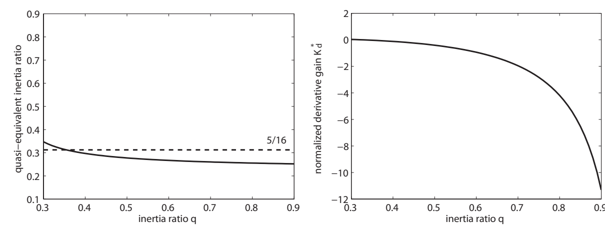

Fig. 7. Analysis of the "resonance ratio control" design. (a) quasi-equivalent inertia ratio. (b) normalized derivative gain K_d^*.

of the drive side ω_m is measurable. Using only the drive velocity feedback, the tendency of pole-zero cancellation at large q's makes it difficult to have a balanced controller design between damping and robustness performances.

B. With load velocity feedback

In real applications, there exist cases where the feedback of both drive and load velocities, ω_m and ω_l is available. Then the equivalent inertia ratio of the two-mass system can be exactly specified using the control structure shown in Fig. 9. With the velocity feedback of both the drive and load sides, the twisting torque T_t generated due to the velocity difference of the drive and load sides can be directly calculated. Therefore the relationship between T_m' and the two velocities, ω_m and ω_l in Fig. 9 can be written as

$$(1+K)T_m' - \frac{KK_s}{s}(\Omega_m - \Omega_l) - \frac{K_s}{s}(\Omega_m - \Omega_l) = J_m s \Omega_m. \tag{25}$$

Eq. (25) can be simplified as

$$T_m' - \frac{K_s}{s}(\Omega_m - \Omega_l) = J_m' s \Omega_m, \tag{26}$$

where

$$J_m' = \frac{J_m}{1+K}. \tag{27}$$

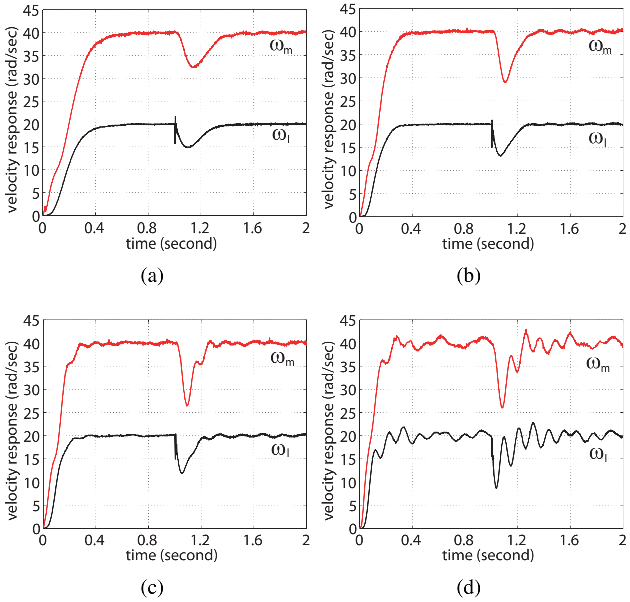

Fig. 8. "Resonance ratio control" without load velocity feedback. (a) $q = 0.3612$. (b) $q = 0.5254$. (c) $q = 0.6752$. (d) $q = 0.7966$.

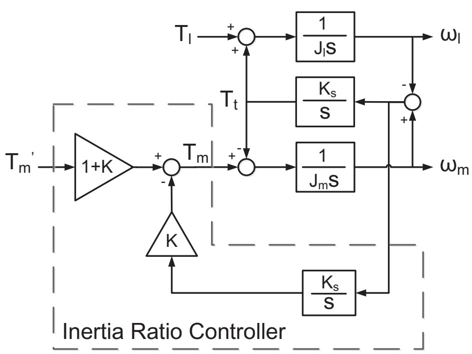

Fig. 9. Block diagram of the inertia ratio control using the feedback of both drive and load velocities.

Since $J_m^{'}$ can be considered as the equivalent inertia of the drive side, the equivalent inertia ratio $q^{'}$ can be defined as

$$q^{'} = \frac{J_m^{'}}{J_m^{'} + J_l} = \frac{q}{1 + (1-q)K}. \tag{28}$$

Namely, an arbitrary inertia ratio $q^{'}$ can be specified by choosing the corresponding value of K.

As discussed in section III, 5/16 is a desirable inertia ratio for the IP control that enables the nominal characteristic ratio assignment [2.5, 2, 2]. By letting the equivalent inertia ratio $q^{'}$ be equal to 5/16, K and the equivalent drive inertia $J_m^{'}$ can be determined as

$$K = \frac{16q - 5}{5(1-q)} \text{ and } J_m^{'} = \frac{5(1-q)}{11q} J_m, \tag{29}$$

respectively. Then, using IP control for the virtual two-mass system, it is straightforward to calculate the real parameters of the IP controller based on Eqs. (10)(12),

$$K_p = K_p^* \frac{J_m^{'} \omega_a}{q^{'}} = \frac{20}{11\sqrt{2}} \sqrt{J_l K_s},$$
$$K_i = K_i^* \frac{J_m^{'} \omega_a^2}{q^{'}} = \frac{4}{11} K_s. \tag{30}$$

Considering the dependence of the above controller design on the nominal value of the spring coefficient K_s, its robustness against spring coefficient variation need be investigated. Real spring coefficient is supposed to be α times of its nominal value, i.e., $K_{s,real} = \alpha K_s$, then Eq. (25) can be modified as

$$T_m^{'} - \frac{(\alpha + K)K_s}{(1+K)s}(\Omega_m - \Omega_l) = \frac{J_m}{1+K} s\Omega_m, \tag{31}$$

namely the two-mass system has an equivalent spring coefficient $K_s^{'}$ as equal as

$$K_s^{'} = \frac{\alpha + K}{1 + K} K_s. \tag{32}$$

As shown in Fig. 10, the variation range of $K_s^{'}$ is limited for a largely varying $K_{s,real}$, especially when the inertia ratio q is large. In addition, the value of spring coefficient K_s only affects the time-scale factor ω_a defined in Eq. (2). The shape of the step time response is irrelevant with K_s.

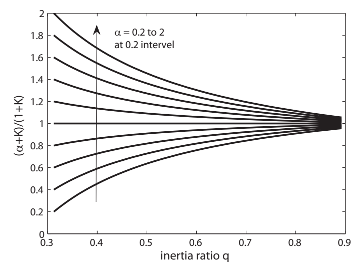

Fig. 10. The ratio of $K_s^{'}$ to K_s versus inertia ratio q.

The inertia ratio control shows an obvious improvement both in terms of damping and robustness performances even at large inertia ratios (see Fig. 11). Furthermore, it has a strong robustness against disturbance torque and spring coefficient variation. As shown in Fig. 12, even the spring coefficient varies 18.4904 times larger, the inertia ratio control still shows a good performance with the controller parameters designed for the original case. By using the feedback of both drive and load velocities, the negative derivative gains in the "resonance ratio control" can be avoided. Therefore the inertia ratio control can maintain both a sufficient damping and a good robustness for large inertia ratios.

V. Conclusion

In this paper, a polynomial-based design of the inertia ratio controllers is discussed for the vibration suppression in two-mass system. Due to the tendency of pole-zero cancellation at large inertia ratios, it is difficult to achieve a balanced controller design between damping and robustness performances using only drive velocity feedback. First, the IP controller is designed based on the nominal characteristic ratio assignment. A desirable inertia ratio of 5/16 is derived at which the IP

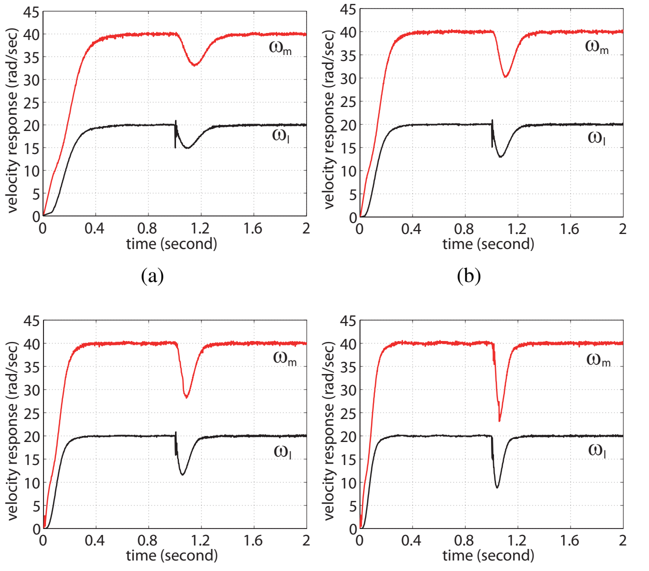

(a) (b) (c) (d)

Fig. 11. Inertia ratio control with load velocity feedback. (a) $q = 0.3612$. (b) $q = 0.5254$. (c) $q = 0.6752$. (d) $q = 0.7966$.

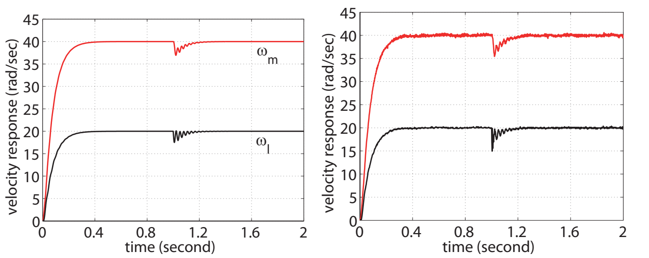

(a) (b)

Fig. 12. Inertia ratio control under the variation of spring coefficient ($q = 0.7966$). (a) Simulation. (b) Experiment.

control provides a proper damping. Two approaches for the control of equivalent inertia ratio are then discussed. The "resonance ratio control" is capable of providing a sufficient damping for large inertia ratios by using only the drive velocity feedback. However, a negative derivative gain, i.e. positive derivative feedback loop, is necessary, which leads to a poor robustness. On the other hand, with the availability of both the drive and load velocity feedback, the equivalent inertia ratio can be exactly specified as equal as its desirable value, 5/16. Without introducing of positive derivative feedback loop, the inertia ratio control structure with load feedback shows both a sufficient damping and a strong robustness for the cases with large inertia ratios.

All the experimental results validated the polynomial-based controller design. The demonstrated generality and the explicit expression of damping by using the polynomial method indicate its promising prospect for solving more complicated control problems.

Acknowledgment

The authors would like to thank National Science Foundation of China, for supporting this work [grant number 50905113 (2010-2012)].

References

[1] Y. Hori, "Future Vehicle Driven by Electricity and Control - Research on Four-Wheel-Motored 'UOT Electric March II'", *IEEE Trans. Ind. Electron.*, vol. 51, no. 5, pp .954-962, October 2004.

[2] E. Omine, T. Goya, U. Akie, T. Senjyu, A. Yona, N. Urasaki and T. Funabashi, "Torsional torque suppression of decentralized generators using H∞ observer", *Renewable Energy*, vol. 35, no. 9, pp. 1908-1913, Sep. 2010.

[3] K. Sugiura and Y. Hori, "Vibration Suppression on 2- and 3- Mass System Based on the Feedback of Imperfect Derivative of the Estimated Torsional Torque", *IEEE Trans. Ind. Electron.*, vol. 43, no. 1, pp. 56-64, Feb. 1996.

[4] K. Lee and F. Blaabjerg, "An Improvement of Speed Control Performances of a Two-mass System Using a Universal Approximator", *Electr Eng*, vol. 89, pp. 389-396, 2007.

[5] R. Dhaouadi, K. Kubo and M. Tobise, "Two-Degree-of-Freedom Robust Speed Controller for High-Performance Rolling Mill Drives", *IEEE Trans. Ind. Appli.*, vol. 29, no. 5, pp. 919-926, Sep./Oct. 1993.

[6] M. Hirata, K.Z. Liu and T. Mita, "Active Vibration Control of a 2-mass System Using μ-Synthesis with a Descriptor Form Representation", *Control Eng. Practice*, vol. 4, no. 4, pp. 545-552, 1996.

[7] S. N. Vukosavić and M. R. Stojić, "Suppression of Torsional Oscillations in a High-Performance Speed Servo Drive", *IEEE Trans. Ind. Electron.*, vol. 45, no. 1, pp. 108-117, Feb. 1998.

[8] Y. Hori, H. Sawada, and Y. Chun, "Slow Resonance Ratio Control for Vibration Suppression and Disturbance Rejection in Torsional System", *IEEE Trans. Ind. Electron.*, vol. 46, no. 1, pp. 162-168, Feb. 1999.

[9] G. Zhang, J. Furusho, "Speed Control of Two-Inertia System by PI/PID Control", *IEEE Trans. Ind. Electron.*, vol. 47, no. 3, pp. 603-609, 2000.

[10] K. Szabat, T. Orlowska-Kowalska, "Vibration suppression in two-mass drive system using PI speed controller and additional feedbacks - comparative study", *IEEE Trans. Ind. Electron.*, vol. 54, no. 2, pp. 1193-1206, 2007.

[11] L. Wang and Y. Frayman, "A dynamically generated fuzzy neural networkand its application to torsional vibration control of tandem cold rolling mill spindles", *Engineering Applications of Artificial Intelligence*, vol. 15, pp. 541-550, 2002.

[12] T. Orlowska-Kowalska and K. Szabat, "Neural-Network Application for Mechanical Variables Estimation of a Two-Mass Drive System", *IEEE Trans. Ind. Electron.*, vol. 54, no. 3, pp. 1352-1364, Jun. 2007.

[13] T. Orlowska-Kowalska, M. Dybkowski, and K. Szabat, "Adaptive Sliding-Mode Neuro-Fuzzy Control of the Two-Mass Induction Motor Drive Without Mechanical Sensors", *IEEE Trans. Ind. Electron.*, vol. 57, no. 2, pp. 553-564, Feb. 2010.

[14] Y. C. Kim, L. H. Keel, and S. P. Bhattacharyya, "Transient Response Control via Characteristic Ratio Assignment", *IEEE Trans. Automatic Control*, vol. 48, no. 12, pp. 2238-2244, Dec. 2003.

[15] Y. C. Kim, L. H. Keel, and S. Manabe, "Controller Design For Time Domain Specifications", in Proceedings of the 15th IFAC Triennial World Congress, Barcelona, Spain, 2002.

[16] P. Naslin, "Essentials of Optimal Control", Cambridge, MA: Boston Technical Publishers, Inc., 1969.

[17] S. Manabe, "Importance of Coefficient Diagram in Polynomial Method", in Proceedings of the 42nd IEEE Conference on Decision and Control, Maui, Hawaii USA, 2003, pp. 3489-3494.

[18] K. A. Folly, "On the prevention of pole-zero cancellation in H∞ power system controller design: A comparison", *South African Institute of Electrical Engineers*, vol. 99, no. 4, pp. 103-113, 2008.

[19] Y. Hori, "A review of torsional vibration control methods and a proposal of disturbance observer-based new techniques", in Proceeding of the 13th IFAC World Congress, San Francisco, July, 1996, pp. 7-13.

[20] C. T. Chen, "Analog and Digital Control System Design: Transfer-function, State-space, and Algebraic Methods", International edition, Saunders College Publishing, 1993.